Chemical Engineering Journal 448 (2022) 137638

Contents lists available at ScienceDirect

Chemical Engineering Journal

journal homepage: www.elsevier.com/locate/cej

Reducing the contact time of impacting water drops on superhydrophobic surfaces by liquid-like coatings

Yue Fan [a,b], Chengjiao Wu [a,b], Jinlong Yang [c], Yingke Wang [a,b], Yi Zhou [a,b], Jiajia Zhou [d], Jia Luo [e], Jun Zhang [e], Shilin Huang [a,b], Xuelin Tian [a,b,*]

[a] State Key Laboratory of Optoelectronic Materials and Technologies, School of Materials Science and Engineering, Sun Yat-sen University, Guangzhou 510006, China
[b] Key Laboratory for Polymeric Composite & Functional Materials of Ministry of Education, Guangzhou Key Laboratory of Flexible Electronic Materials and Wearable Devices, Sun Yat-sen University, Guangzhou 510006, China
[c] Institute of Fundamental and Frontier Sciences, University of Electronic Science and Technology of China, Chengdu 610054, China
[d] School of Emergent Soft Matter, South China University of Technology, Guangzhou 510640, China
[e] School of Aeronautic Science and Engineering, Beihang University, Beijing 100191, China

ARTICLE INFO

Keywords:
Superhydrophobic surfaces
Contact time
Drop impact
Liquid-like coatings
Dynamic liquid repellency

ABSTRACT

Surfaces that can rapidly shed impacting drops are important for a wide range of applications, including anti-icing, dropwise condensation and miniaturized drones. Previous strategies to reduce the contact time of impacting drops are primarily based on engineering superhydrophobic surfaces through introducing secondary textures, either macroscopic or nanoscopic, or constructing specifically designed nanotextures. Here, a facile and effective approach is demonstrated to reduce the contact time of superhydrophobic surfaces by simply replacing the widely used perfluorosilane (i.e., trichloro (1H, 1H, 2H, 2H-perfluorooctyl) silane, PFOS) coating with liquid-like perfluorinated polyether (PFPE) surface chemistry. Though their apparent contact angles are comparable, the PFPE-coated superhydrophobic surface exhibits a reduction of contact time up to 26% compared to the PFOS-coated counterpart, attributed to enhanced retraction speed on the former surface. Remarkably, while a classical inertial model predicts a merely 3% difference in retraction time between the PFPE- and the PFOS-coated surfaces, a drastic reduction of retraction time by 12–32% is observed. The improved retraction dynamics on the liquid-like surface is suggested to be caused by the low contact angle hysteresis and enhanced interface slippage on the liquid-like coating. This study offers a general strategy to enhance dynamic liquid repellency of superhydrophobic surfaces for diverse applications.

1. Introduction

Drop impact on superhydrophobic surfaces has recently attracted extensive attentions for the significance in a wide variety of fundamental and industrial research areas, such as self-cleaning of plants [1–4], survival of insects in heavy rains [5–7], anti-icing of airframe [8–10], drop-based heat transfer [11,12] and energy harvesting [13–15]. *Richard* et al., [16] quantified in 2002 the contact time of drop impact on water-repellent surfaces based on inertial-capillary balance as $t_c = a(\rho D^3/8\gamma)^{1/2}$, where t_c is the contact time, a is a prefactor determined experimentally, and ρ, D, γ are the density, diameter, and surface tension of the liquid drop, respectively. Since then, a range of strategies have been explored to achieve a reduced contact time below the theoretical limit. A well-known method is introducing macrotextures to micro/nanotextured superhydrophopic surfaces [17,18]. The macrotexture can redistribute the drop mass and induce a non-axisymmetric recoil of the contact line, enabling drop rebound with an impressive contact time reduction. Symmetry breaking in drop bouncing also occurs on superhydrophobic surfaces with macroscopic curved morphology (e.g., *Echevaria* leaves), which allows asymmetric momentum and mass

* Corresponding author.
E-mail address: tianxuelin@sysu.edu.cn (X. Tian).

https://doi.org/10.1016/j.cej.2022.137638
Received 21 February 2022; Received in revised form 26 May 2022; Accepted 16 June 2022
Available online 18 June 2022

distribution and a consequent reduction in contact time [19]. Excitingly, pancake bouncing, noted by *Liu* et al., exhibited a particular rapid drop detachment in the absence of drop recoiling [20]. This is achieved by imprinting superhydrophobic nanotextures on submillimetre-scale post arrays, which can effectively rectify the surface energy of deformed drops into upward liquid motion. More recently, *Wang* et al., demonstrated the availability of shortening the contact time through employing compact nanoscale textures with size down to 100 nm on superhydrophobic surfaces of high solid fraction, in which the effect of line tension driven by the high contact line density promotes fast drop rebound [6].

Despite the above tremendous progress, the reported methods are primarily based on tuning the surface structures of superhydrophobic surfaces by introducing secondary textures, either macroscopic or nanoscopic, or constructing compact nanostructures of specific sizes. This makes the fabrication inevitably relies on tedious fabrication procedures or particular structure design. Moreover, some surfaces requires the drop to impact on certain position (e.g., the macrotextures) to minimize the impact duration, which would to some extent limit their applicability. A facile and general strategy capable of shortening contact time of superhydrophobic surfaces is thus in high demand. Among the diverse superhydrophobic surfaces, fluorinated coatings, such as PFOS, are widely adopted for low-surface-energy functionalization. Herein we show that a liquid-like PFPE coating featuring highly flexible molecular chains can effectively reduce the impact duration of drops on superhydrophobic surfaces by enhancing their retraction dynamics. As a type of grafted flexible polymer brush emerging over the last few decades, liquid-like coatings exhibit exceptional and stabilized dynamic liquid-repellency [21–24]. Previous studies on liquid-like coatings have paid much attention to their intrinsic omniphobicity as well as ultra-low hysteresis towards sessile drops [23,25]. In this paper, we investigate, for the first time, to use liquid-like coatings to reduce the contact time of impacting drops on superhydrophobic surfaces. The novelty of our strategy is that the contact time can be effectively reduced by simple surface modification with liquid-like coatings, and it is no longer necessary to design complex and specific surface textures. Furthermore, while a classical inertia model predicts a slight difference of 3% in retraction time between the PFOS- and the PFPE-coated surfaces, we observe an at least fourfold increase in this time difference, attributed to the low contact angle hysteresis and the interface slippage of the liquid-like coating.

2. Results and discussion

It is well known that superhydrophobic surfaces can be made by combining rough surface textures with low-surface-energy chemical modification [26–33]. In this study, we used a micro-fabrication approach to pattern micropillars on a silicon substrate, and coated it with liquid-like PFPE polymer brushes (Fig. 1a). Scanning electron microscopy (SEM) image showed the uniform topography on the surface (Fig. 1b). All the micropillars were cylindrical with a diameter D_p of 10 μm, and were arranged in square lattices with a centre-to-centre spacing L_p of 20 μm, corresponding to $\phi_s = 0.20$ where $\phi_s = \pi D_p^2 / 4L_p^2$ is the area fraction of the solid in contact with the liquid (i.e., the solid fraction). Noted that an increased ϕ_s can be achieved by designing more compact pillar arrays, and vice versa. The PFPE polymer features highly flexible molecular chains, characterized by its extremely low glass transition temperature (-116 ℃) [22,34]. At the molecular scale, the torsional barrier of its repeated C-O-C bonds was comparable to the energy of thermal motion, leading to a variable dynamic molecular conformation [25,35]. As a consequence, the PFPE molecular chains behave like a liquid at room temperature when covalently grafted onto a solid substrate (Fig. 1c). In previous studies, we have found that a liquid-like coating can enhance liquid repellency of non-wetting surfaces by suppressing microscopic liquid residue when a drop moves away from the surface [36,37]. This inspires us to explore whether such coating can help to minimize the contact time of an impacting drop on superhydrophobic surfaces. A control sample was also prepared by applying conventional PFOS coating onto the microfabricated surface with the same structure (Fig. 1a, d). The successful grafting of PFPE and PFOS was confirmed by X-ray photoelectron spectroscopy (Fig. 1e). The specific C-O-C bonding in PFPE polymer chains was identified by the O1s XPS spectra (Fig. 1f). Although the PFPE- and the PFOS-coated micropillared surfaces are both superhydrophobic with similar static contact angles θ_s (159° and 157°, respectively, Fig. 1c-1d), their advancing and receding contact angles are distinct (Table S1). The PFPE-coated surface

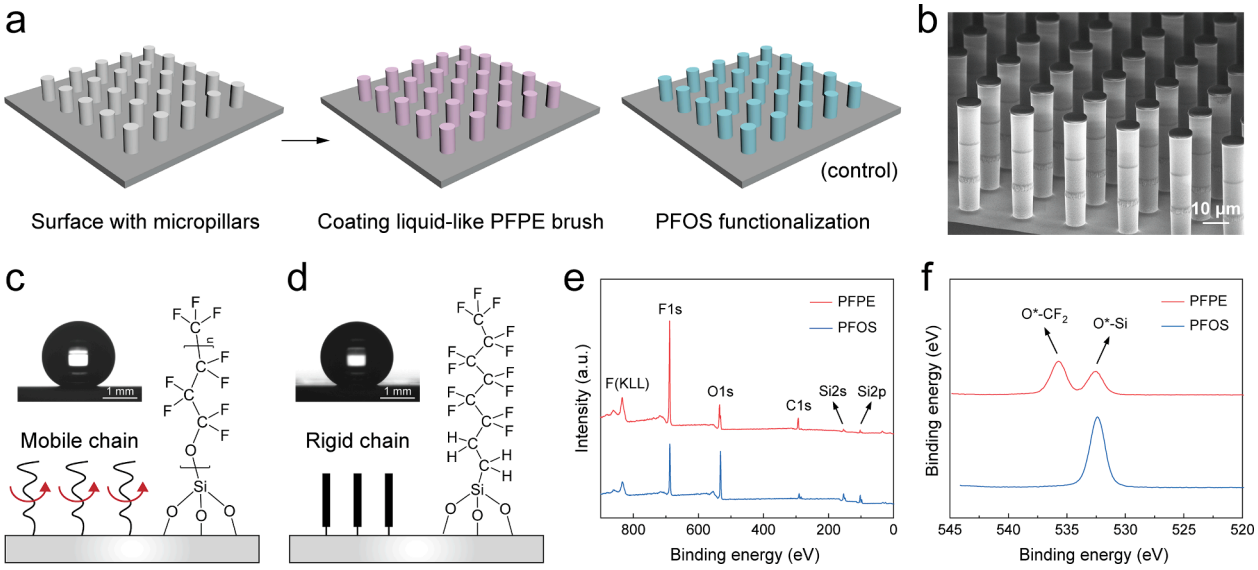

Fig. 1. Surface preparation and characterization. a) Schematic of the prepared micropillared surface coated with liquid-like PFPE brushes and the control sample coated with PFOS. b) SEM image of the prepared surface with top diameter of pillars $D_p = 10$ μm, height $H = 45$ μm and surface solid fraction $\phi_s = 0.20$. c) Schematic of the tethered PFPE molecule on the surface with high molecular mobility. The contact angle, contact angle hysteresis and sliding angle on the PFPE-coated micropillared surface were 159°, 26° and 5.2°, respectively. d) Schematic of rigid PFOS molecule tethered on the surface as a control sample. The corresponding contact angle, contact angle hysteresis and sliding angle were 157°, 37° and 10.6°, respectively. e,f) XPS spectra and the O 1 s spectra of the surfaces coated with PFPE and PFOS.

exhibits much lower contact angle hysteresis (i.e., the difference between the advancing and the receding contact angles) and sliding angle than the PFOS-coated one, a typical characteristic of liquid-like coating.

To investigate how the liquid-like coating differs from conventional perfluorosilane coating in affecting the contact time of bouncing drops on superhydrophobic surfaces, water drops with diameters of 2.15 mm (±0.5%) were let to impact on the prepared surfaces with a velocity of 0.48 m/s, corresponding to We = 6.8 (We = $\rho Dv^2/\gamma$ is the Weber number, and v is the impact velocity). This We was first chosen to demonstrate the impact dynamics as the liquid-like coating displayed significant advantages in contact time reduction under such condition. A high-speed camera at the rate of 10,000 frames per second was utilized to observe the drop bouncing processes, and the selected side-view snapshots were shown in Fig. 2a. While negligible distinctions were observed at the spreading stage, the retraction phase was pronouncedly influenced by the surface chemistry. The drop retracted gently on the PFOS-coated surface and detached from the surface at 14.5 ms. By contrast, on the PFPE-coated sample, the contact line retracted much more trippingly and the drop bounced off the surface within 10.7 ms (Video S1). The simple replacement of perfluorosilane coating with liquid-like coating thereby led to a contact time reduction of ~ 26%.

To explore the dynamics of impacting drops, we measured the normalized contact diameter D_c/D_0 (D_c is the contact diameter and D_0 the initial diameter of the drop) as a function of time for both surfaces (Fig. 2b). The two series of contact diameters coincide in the whole spreading process, and reach the maximum lateral extension synchronously at ~ 2.4 ms. This is in accordance with previous reports, which indicated that the spreading process is primarily determined by the kinetic energy of the impacting drop [38,39]. However, during the retraction stage, the contact diameter for the PFPE-coated surface is always below that for the PFOS-coated surface, and the drop retraction speed, characterized as the slope of the contact diameter plots, exhibits a greater value on the former surface. Note that the plots were not smooth at a few points. This was commonly seen in modest-We drop impact, in which the capillary wave propagation cannot be neglected [40].

The contact time t_c of a bouncing drop on water-repellent surfaces scales with the inertia-capillary time scale and obeys the following equation [16],

$$t_c = a\left(\rho D^3/8\gamma\right)^{1/2} \quad (1)$$

We investigated the size-dependent contact time on the two surfaces using drops of different volumes (Fig. 2c), and the results are in well agreement with the scaling law of Eq. (1). On the PFPE-coated surface, the fitting curve gives a prefactor of $a = 2.7$, which is smaller than that on the PFOS-coated control surface with $a = 3.6$. This is unexpected for drops bouncing on non-wetting surfaces made of micron-scaled structures. Previous works have shown the prefactor is profoundly influenced by the dimension of surface texture [17,19,20,41–47] (Fig. 2d). In an ideal condition of a freely oscillating drop, the prefactor is dictated by the Rayleigh time formula $t_{Rayleigh} = 2^{-1/2}\pi(\rho D^3/8\gamma)^{1/2}$ as $a \approx 2.2$ [48]. On nano-textured non-wetting surfaces with low solid fraction f_s, prefactor values closed to 2.6 were reported in a majority of relevant researches [19,20,45–47]. This increase could be attributive to the restricted vibration of droplets on the solid part of surfaces. When the surface structures were amplified to micron level, the prefactor would further increase to at least 3.1, and even up to 3.8 in some reports [17,41–44]. In our study, the prefactor $a = 3.6$ of the micropillared surface with conventional PFOS coating was indeed among the reported range for solely microstructured superhydrophobic surfaces. Notably,

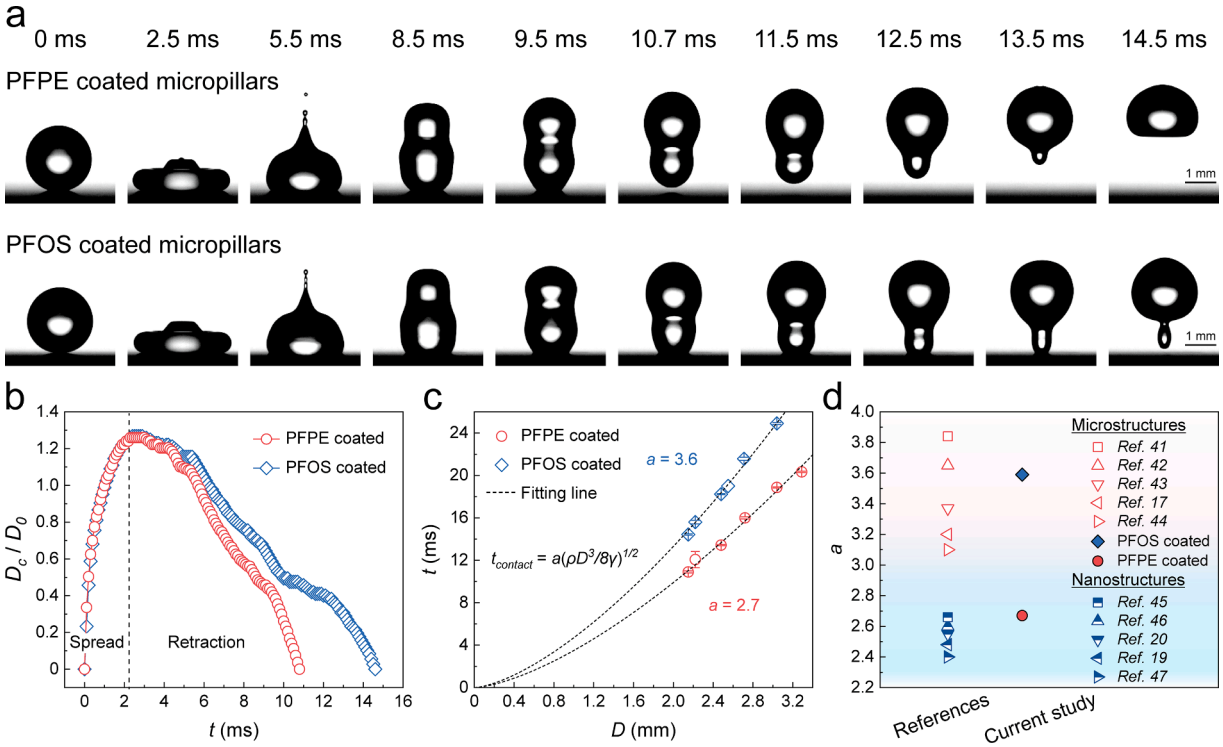

Fig. 2. Comparison of contact time of impacting drops on the PFPE- and the PFOS-coated microtextured surfaces. a) Selected snapshots showing droplets impacting on the PFPE- and PFOS-coated micropillars with solid fraction $\phi_s = 0.20$ at We = 6.8. The droplet bounced off the PFPE-coated micropillars within 10.7 ms, while it detached from the PFOS-coated control sample at 14.5 ms. b) Temporal evolution of the normalized contact diameter D_c/D_0 (D_c is the contact diameter and D_0 the initial diameter of the drop). c) Curves showing the contact time as a function of the drop diameter. According to the equation of the drop contact time on water-repellent surfaces $t_c = a(\rho D^3/8\gamma)^{1/2}$, the prefactor a for the PFPE- and the PFOS-coated surface were fitted as 2.7 and 3.6, respectively. d) Comparison of the prefactor a of superhydrophobic surfaces with micron-scale and nano-scale structures. In the current study, while the PFOS-coated micropillared surface exhibits a prefactor of 3.6, in accordance with previous reports on microstructured superhydrophobic surfaces, the PFPE-coated micropillared surface achieves a greatly reduced prefactor of 2.7, which is comparable to that of the nano-structured surfaces in previous publications.

the prefactor on the same microstructured surface with liquid-like PFPE coating is reduced to 2.7, which is comparable to that of nano-structured superhydrophobic surfaces. This makes the liquid-like PFPE coating highly promising to replace traditional perfluorosilane coating in diverse applications of non-wetting surfaces to minimize the contact time of impacting drops. Moreover, in practical scenarios, while maintaining a similar low-level drop contact time, the slender and fragile nanotextures could be substituted by robust microtextures to promote the mechanical durability of non-wetting surfaces.

To investigate whether the contact time reduction enabled by liquid-like PFPE coating is a general phenomenon, we studied the drop impacting dynamics at a wide range of We conditions with a drop velocity up to 1.31 m/s (corresponding to We = 50.7). Above 1.31 m/s, a Cassie-to-Wenzel transition would occur on the microtextured surfaces as the water hammer pressure would exceed the breakthrough pressure of the micropillars (Fig. S1). Fig. 3a shows the snapshots of drop bouncing on the PFPE- and the PFOS-coated surfaces at We = 50.7. Both surfaces exhibit similar spreading behaviors and reach almost identical maximum spreading diameters D_{max} at 2.4 ms. However, their retraction behaviors are distinct, which lead to notable difference in the contact time. A drop lifted off the PFPE-coated micropillars within 11 ms (corresonding to a prefactor $a \approx 2.7$ in the inertia-capillary time scale), significantly faster than that on the PFOS-coated surface of 12.7 ms (corresonding to a prefactor $a \approx 3.1$). The plots of time-dependent normalized contact diameter are shown in Fig. 3b. Note that the plot for the PFPE-coated surface is fairly smooth, demonstrating an approximately constant retraction speed, whereas for the PFOS-coated surface a less steep plateau is present at about 9 to 12 ms. Further investigations indicate that the PFPE-coated surface always gives greatly reduced contact time than the PFOS-coated one with We numbers from 3.8 to above 50 (Fig. 3c), confirming the universality of using liquid-like coating to suppress the contact duration. Via monitoring the detailed impact dynamics, we were able to resolve the contact time into the spreading and the retraction components. The two surfaces exhibit almost no difference in the spreading time at the same We (Fig. 3d). The retraction time of the PFPE-coated surface is markedly less than the PFOS-coated counterpart at whatever We (Fig. 3e), which consequently leads to the observed difference in the total contact time between the two surfaces.

A classicial inertial mode developed by *Bartolo* et al., [49] could be attempted to analyse the drop retraction dynamics after impacting. A drop impacting a surface at high velocity first deforms to a uniform film at the point of maximum spreading. The capillary force acted on the upper and the bottom sides of the film would then drive the edge to recoil inwards, leading to a retracting rim and a stationary central film [40,50]. Balancing the capillary tension from the film with the inertia of the rim, the retraction speed V_{ret} can be expressed as follows:

$$V_{ret}/D_{\max} \sim \left[\pi\gamma(1-\cos\theta_{\rm rec})/\rho D^3\right]^{1/2} \quad (2)$$

where θ_{rec} is the receding contact angle. According to this scaling law, the receding contact angle seemed to be responsible for the observed difference in the retraction time τ_{ret} (estimated by $\tau_{ret} = D_{max}/V_{ret}$). It is similar to what was observed by *Antonini* et al [51]. Here we define a reduction factor of retraction time $\Delta k = (\tau_{ret\text{-}PFOS} - \tau_{ret\text{-}PFPE})/\tau_{ret\text{-}PFOS}$, in which $\tau_{ret\text{-}PFOS}$ and $\tau_{ret\text{-}PFPE}$ are the retraction time on the PFOS- and the PFPE-coated micropillars, respectively. A higher degree of reduction in contact time would thus give a larger Δk. The receding contact angle of the PFPE- and the PFOS-coated microtextured surfaces are 146° and 135°, respectively (Table S1). Substituting the above contact angles into the above inertial model, a minute Δk of 3% is obtained. Remarkably, the experimentally measured Δk values are drastically larger than the theoretical reduction factor. As shown in Fig. 3f, a lowest Δk of 12% is observed while the highest one is even up to 32% in our experiments. That is, the reduction factors of retraction time between the PFPE- and the PFOS-coated surfaces show an at least fourfold increase compared to

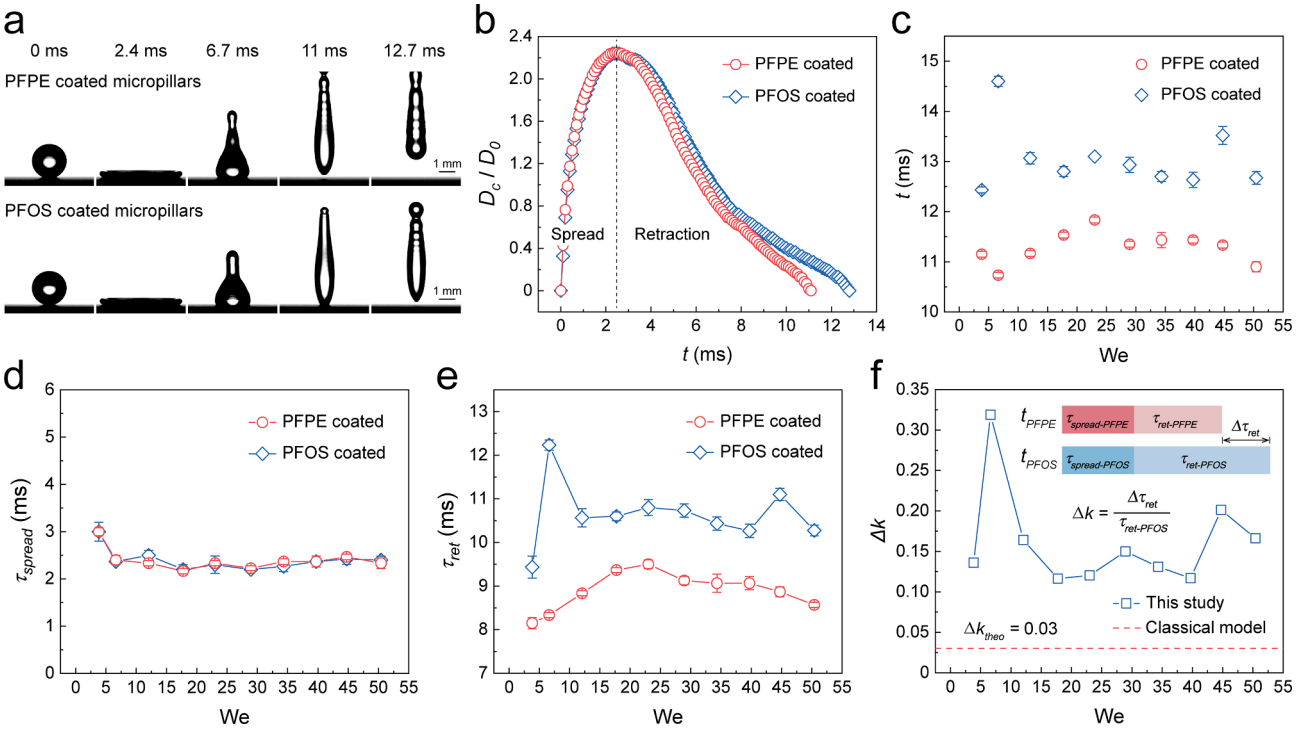

Fig. 3. Investigation of contact time and its spreading and rectraction components at different We, and the mechanism analysis. a) Selected snapshots of droplets hitting on the PFPE- and the PFOS-coated micropillars at We = 50.7. The surface solid fraction ϕ_s is 0.20. b) Plots of the time-dependent normalized contact diameter for the two surfaces. c) Contact time of impacting drops on the the two surfaces at different We. d) Spreading and e) retraction time on the two surfaces. f) Variation of the reduction factor of retraction time Δk at varied We. Here $\Delta k = (\tau_{ret\text{-}PFOS} - \tau_{ret\text{-}PFPE})/\tau_{ret\text{-}PFOS}$, where $\tau_{ret\text{-}PFOS}$ and $\tau_{ret\text{-}PFPE}$ are the retraction time on the PFOS- and the PFPE-coated micropillars, respectively. The theoretical decrease Δk_{theo} predicted by classical inertial model is shown in (f) as the red dotted line.

the classical inertial model.

The huge discrepency between the experimental and the theoretical Δk values suggests that, beyond the receding contact angle, the liquid-like PFPE coating offers extra advantages to promote drop retraction on the surface. Investigations of drop impacting behaviors on flat surfaces also confirm that liquid-like coatings can bring enhanced retraction dynamics beyond that predicted by the classical model (Fig. S2). The drop retraction dynamics can also be understood from an energetic perspective. As mentioned above, the drop spreads to a uniform film at the time of maximum spreading (Fig. S3), which corresponds to a point of maximum surface energy. This surface energy then drives the recoiling of the peripheral rim by transforming the surface energy to kinetic energy. In fact, the term $\gamma(1\text{-}cos\theta_{rec})$ in Eq. (2) could be interpreted as the surface energy per unit area of the liquid film, though strictly the receding angle θ_{rec} should be replaced by thermodynamically most favorable apparent contact angle of the surface (which is in practice difficult to measure). This is why the surface contact angle dominates the retraction dynamics according to the classical inertial model. The minimization of the surface energy provides the driving force for the drop retraction.

However, energy dissipation also takes place at the retraction stage. If energy is well dissipated during drop recoiling, the transform of the surface energy to the kinetic energy would become less effective, leading to reduced retraction speed. We infer that the liquid-like PFPE coating can effectively mitigate the energy dissipation of a retracting drop compared to conventional perfluorosilane coating. Firstly, it is known that the liquid-like coating possesses minimal pinning force towards the solid–liquid-gas triple-phase contact line, often described as extremely low contact angle hysteresis [22,23,34]. The PFPE coating indeed shows lower contact angle hysteresis than the PFOS coating (Table S1, S2). The minimial pinning force of the PFPE coating is thus expected to reduce the interface energy dissipation throughout the contraction of the contact line on the surface. Drop rebounding experiments at very low We confirm much lower interface energy dissipation of the PFPE-coated micropillars compared to the PFOS-coated micropillars (Fig. S4). It is found that a drop impacting the former surface at a low We of 0.97 can rebound for multiple times, whereas on the latter surface the drop only oscillates and can not detach from it. The observed difference could be attributed to the reduced interface energy dissipation of the PFPE-coated surface as viscous dissipation at such low impact velocity is neglegible. Secondly, recent studies suggested that the liquid-like coating could introduce additional interface slippage with increased slip length through its unique lubrication effect [36]. This means that the boundary liquid layer is less constrained by the solid surface and thus able to move more synchronously with the bulk fluid. Decreased viscous dissipation could thus be present on the PFPE-coated surface during drop retraction in the case of drop impacting at relatively high velocity. Taken together, the liquid-like coating are expected to reduce the energy dissipation effectively during drop recoiling and thereby facilitate achieving a higher drop retraction speed.

The reduced energy dissipation on the PFPE coating relative to the PFOS coating is also verified by additional control experiments. As shown in Fig. S5, when a drop impacts a flat PFPE-coated surface at We = 3.8, the contact line retracts rather smoothly, and moreover the drop can finally bounce off the surface swiftly (Fig. S5 and Video S2). In contrast, on the PFOS-coated flat surface the contact line retracts rather

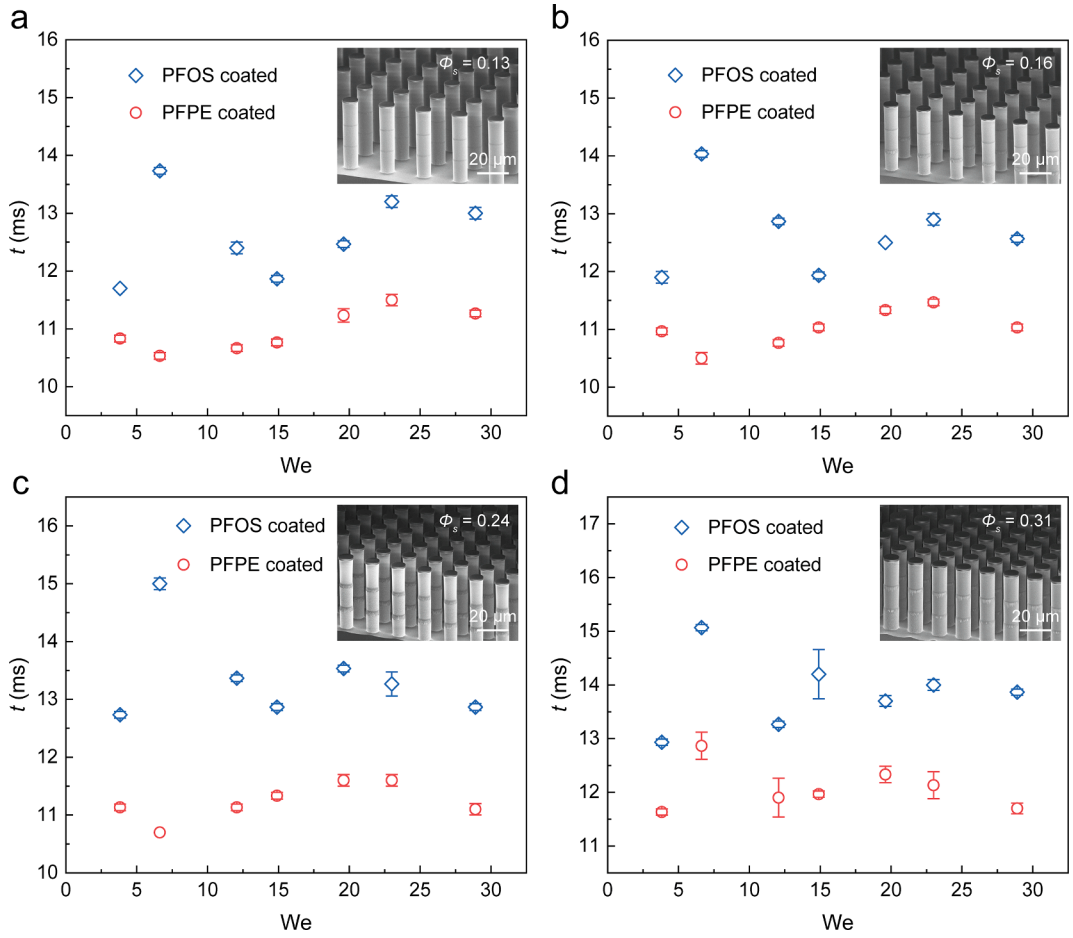

Fig. 4. The ability of liquid-like PFPE coating to reduce the contact time of non-wetting surfaces with varied surface solid fraction ϕ_s. a-d) Comparison of the contact time of impacting drops on the PFPE- and the PFOS-coated micropillars at different We with solid fraction ϕ_s of (a) 0.13, (b) 0.16, (c) 0.24 and (d) 0.31, respectively. The insets in each figure show the SEM images of the corresponding microtextured surfaces.

primly for an impacting drop of the same We, and the drop ultimately gets firmly pinned on the surface. Clearly, the former coating presents both enhanced contact line mobility and reduced energy dissipation. The less energy dissipation of the liquid-like coating is also demonstrated on the microtextured surface by the larger drop rebounding height on the PFPE-coated micropillars relative the PFOS-coated counterpart (Fig. S6).

We further verified the ability of the liquid-like coating in reducing the contact time of non-wetting surfaces with various solid fractions (Fig. 4). A range of microtextured surfaces with solid fraction ϕ_s varied from 0.13, 0.16, 0.24 to 0.31 were employed in the investigation. For whatever solid fraction, the contact time of impacting drop on the PFPE-coated surface is always less than that on the FPOS-coated one, regardless of the We. Though the classical inertial model still predicts negligible difference in the contact time between the two surfaces, the experimentally observed difference is noteworthy, similar to the case of drop impacting on the microtextured surface with $\phi_s = 0.20$.

Additionally, to demonstrate the strategy of using liquid-like coatings to reduce contact time of impacting drops is applicable to liquids with different surface tensions and viscosities, we performed a series of experiments using ethylene glycol and its water solutions as the probe liquids. As expected, the PFPE-coated superhydrophobic surface always showed a significantly reduced contact time than the PFOS-coated counterpart for all the investigated liquids (Fig. S7), regardless of their surface tensions,viscosities and drop sizes (Table S4).

Finally, to demonstrate whether the reduction of contact time of impacting drops was a universal effect for liquid-like surface chemistry, we extended our studies to another well-known liquid-like coating, i.e., the linear polydimethylsiloxane (PDMS) brush coating (Fig. 5). Analogus to the PFPE, the PDMS polymer has an extremely low glass transition temperature (-127℃) and features highly flexible molecular chains [21]. The PDMS brush coating can thereby also behave as a liquid-like layer at room temperature [52–56]. We applied the liquid-like PDMS coating onto the microtextured surface with $\phi_s = 0.20$ and compared its drop impacting behaviors with the PFOS- and the PFPE-coated micropillars. The successful grafting of PDMS brush coating is verified by XPS analyses (Fig. S8). Interestingly, the PDMS-coated surface shows similar wetting property to the PFOS-coated one (Fig. 5a and Table S1), and their receding contact angles are identical to be 135°. The equivalent wettability of the two surfaces allowed us to better resolve the influence of liquid-like features on drop impacting dynamics. Fig. 5b compares the drop bouncing behaviors on the PDMS-, the PFPE- and the

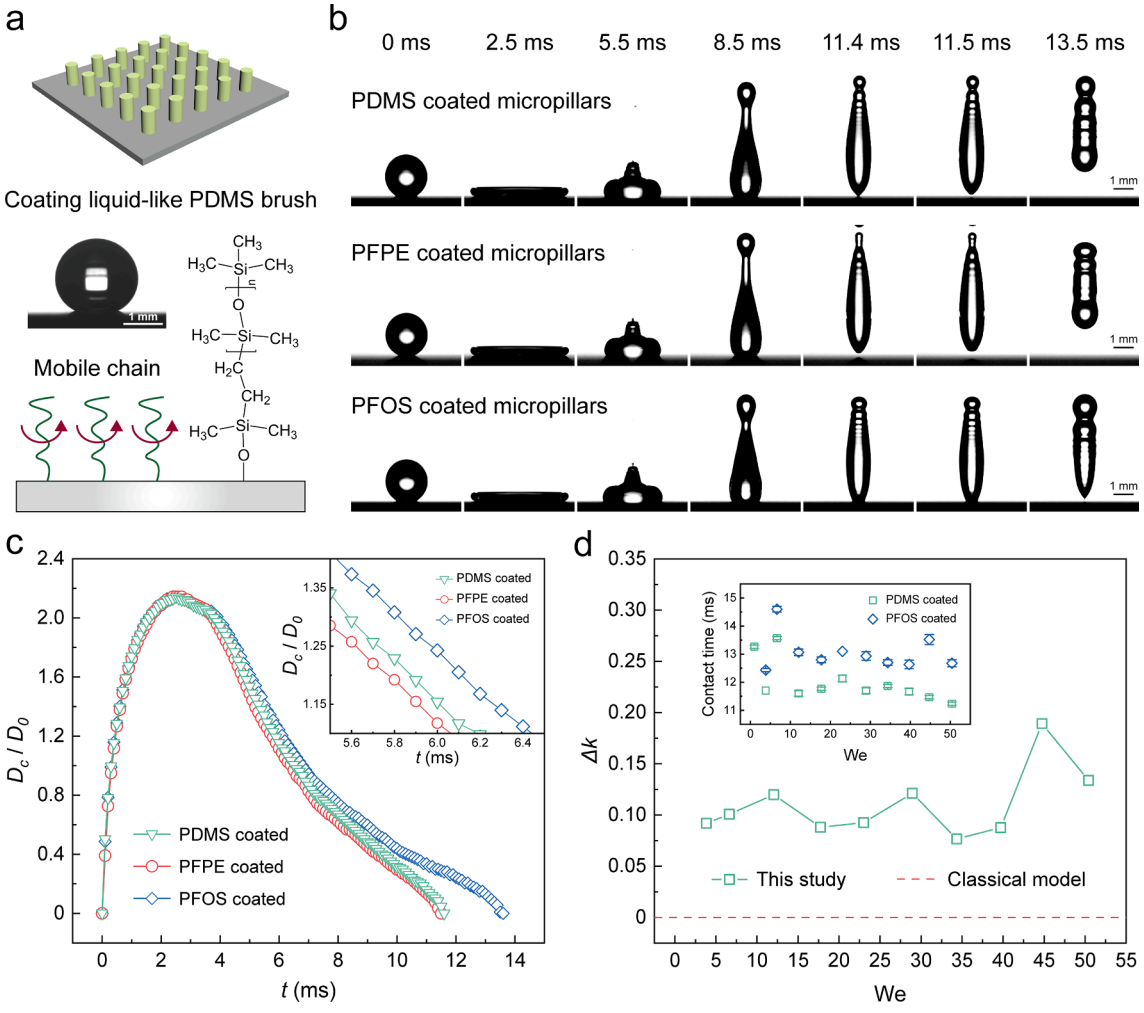

Fig. 5. Demonstration of contact time reduction by the PDMS brush coating, which is another well-known liquid-like coating. a) Schematic of the liquid-like PDMS brushes coated on the micropillared surface. The contact angle, contact angle hysteresis and sliding angle on the PDMS-coated micropillars with $\phi_s = 0.20$ were 157°, 37° and 7.7°, respectively. b) Selected snapshots showing drop impacting behaviors on the PDMS-, the PFPE- and the PFOS-coated micropillars at We = 44.7. The corresponding contact time was 11.5 ms, 11.4 ms and 13.5 ms, respectively. c) Curves of time-dependent normalized contact diameters of impacting drops on the three surfaces. d) Variation of the reduction factor of retraction time Δk at varied We. Noted that Δk here was defined as $\Delta k = (\tau_{ret\text{-}PFOS} - \tau_{ret\text{-}PDMS}) / \tau_{ret\text{-}PFOS}$, where $\tau_{ret\text{-}PFOS}$ and $\tau_{ret\text{-}PDMS}$ are the drop retraction time on the PFOS- and the PDMS-coated micropillars, respectively. The inset compares the droplet contact time on the two surfaces at varied We.

PFOS-coated micropillars at We = 44.7. While the impinging drops reached their maximum lateral extensions at the same time of 2.5 ms on the three surfaces, their retraction processes make a difference (Video S3). The drop on the PDMS-coated surface recoils almost as fast as that on the PFPE-coated one, giving to a comparable contact time (11.5 ms for the former and 11.4 ms the latter). In contrast, on the PFOS-coated micropillars a much larger contact time of 13.5 ms is obtained. That is, the PDMS coating shows similar capability to reduce the contact time to the PFPE. The curves of time-dependent normalized contact diameters for the three surfaces are plotted in Fig. 5c. The contact diameters for the PDMS-coated surface are in between the other two sets of values with a tendency to approach those of the PFPE-coated sample (inset in Fig. 5c). In particular, a gradually increased gap between the curves of the PFOS-coated surface and the other two can be observed with prolonged recoiling time, highlighting the distinction between the liquid-like coatings and the conventional perfluorosilane coating. We further measured the contact time of impacting drops on the PDMS- and the PFOS-coated surfaces at varied We and analyzed the corresponding reduction factor of retraction time Δk between the two surfaces (Fig. 5d). Note that according to classcial inertial model the PDMS- and the PFOS-coated surfaces should have the same retraction time due to their identical receding contact angles (Table S1), and the theoretical reduction factor Δk_{theo} should thus be 0. However, the experimental reduction factor Δk at various We are calculated to be among 8% and 19%. These facts further confirm that, beyond the receding contact angle, the liquid-like coatings indeed bring about unique advantages in shortening the contact time of impacting drops by reducing the energy dissipation during drop retraction.

3. Conclusion

In summary, we experimentally show that the liquid-like brush coatings featuring highly mobile molecular chains are dramatically conducive to reduce the contact time of a bouncing drop on superhydrophobic surfaces. Compared to traditional perfluorosilane coatings, the liquid-like PFPE and PDMS coatings greatly enhanced the retraction dynamics of impacting drops on the microtextured non-wetting surfaces. In particular, the measured reduction factors of retraction time at varied We are far beyond the theoretical values that are predicted by the classical inertial model. We suggest that the low contact angle hysteresis and the interface slippage of the liquid-like coating effectually reduce the energy dissipation during drop recoiling, thus facilitate the achievement of unthought-of performance in enhancing the drop retraction dynamics. Our study offers a general and effective strategy to reduce the contact time of impacting drops on non-wetting surfaces based on simple surface modification. Moreover, by combining previously reported structure engineering approaches [6,17–20] with liquid-like surface chemistry, non-wetting surfaces with extremely low contact duration to impacting drops are expected to be created. Such surfaces could realize unprecedented lower drop contact time than existing surfaces, which are highly attractive to scenarios demanding ultrafast drop shedding. We believe the above findings are of great importance to develop functional surfaces of excellent dynamic drop repellency with widespread application prospects in anti-icing, heat transfer, energy harvesting and miniaturized air vehicles.

4. Experimental section

4.1. Fabrication of microtextured surfaces

The textured surfaces with cylindrical micropillars were fabricated by combining photolithography with deep reactive ion etching (DRIE). First of all, a 500 μm-thick silicon wafer with 2 μm-thick SiO_2 top film was selected as the substrate. A layer of photoresist AZnLOF 2035 (MicroChemicals, GmbH), with thickness of 1.9 μm measured by the step profiler (AlphaStep D-120, KLA-Tencor), was then spin-coated on the substrate. The micropattern was designed by the Klayout sofware, and was lithographed to the photoresist layer by the UV-light exposure in a uPG501 mask writer (Heidelberg Instruments). After development and post-baking, a 2 μm deep anisotropic SiO_2 etching (Table S5, recipe 1 in Supporting Information) was conducted by the DRIE system (Oxford Instruments, PlasmaPro 100 Estrelas) to transform the pattern onto the SiO_2 top film. The remaining photoresist was further removed by ultrasonic cleanout in acetone and oxygen plasma cleaning. Ultimately, ultilizing the SiO_2 pattern as a hard mask, a 45 μm deep Si post array was achieved by a 240-loop DRIE Bosch Process (Table S6, recipe 2 in Supporting Information). The surface was ready for further functionalization after a second oxygen plasma cleaning, and the remaining SiO_2 top cap was not required to be removed so that we could adjust the ϕ_s to designed values precisely.

4.2. Surface functionalization

i). PFPE coating. The PFPE brush layer was coated on the microtextured surface and the smooth surface through the following method. First, the as-fabricated surface was plasma-treated for 5 min using an oxygen plasma cleaner (Harrick Plasma, PDC-002, O_2 flow rate = 15 sccm, RF power = 30 W). Then, it was dip-coated by a 0.5 wt% solution of trimethoxysilyl-terminated PFPE (Optool, Daikin) in Novec 7200, followed with a 5 min solvent evaporation in air (25 Deg, relative humidity ~ 50%). To achieve a firm grafting, the surface was subsequently annealed at 130℃ for 30 min. Ultimately, the PFPE-coated surface was soaked in hexane for 2 h for a thorough cleaning.

ii). PFOS coating. A simple approach of chemical vapor deposition (CVD) was used to coat PFOS. First, the as-fabricated surface underwent a similar oxygen plasma treatment as mentioned above. It was then placed into a vacuum desiccator together with an open glass vessel containing about 0.2 mL 1H,1H,2H,2H-perfluorooctyltrichlorosilane (PFOS, Sigma Aldrich, 97%). The vacuum was kept at ~ − 0.09 MPa for 2 h to guarantee a complete silanization reaction. The PFOS-coated surface was finally obtained after vacuum venting and volatilization of unreacted silane residues.

iii) PDMS coating. The linear PDMS brush layer was covalently tethered on the microtextured surface and the smooth surface by a two-step synthetic route (Fig. S6). As a preprocessing, the as-fabricated surface was treated by oxygen plasma with the same parameters mentioned above. The first step was grafting of double bond groups on the surface. The hydroxyl groups on the plasma-treated surface was let to react with 0.4 mL chlorodimethylvinylsilane (TCI, 97%) for 5 min in a 50 mL beaker containing 20 mL dichloromethane (General-Reagent, AR), catalyzed by 25 mg 4-dimethylaminopyridine (Adamas-beta, 99%) and 0.8 mL triethylamine (Adamas-beta, 99%). After cleaning by ethanol and deionized water, the surface performed the second-step reaction to tether PDMS molecules. A mixed solution of 0.6 mL monohydride terminated polydimethylsiloxane (PDMS, Gelest, 5–8 cSt) and 15 μL Karstedt catalyst solution (Meryer, Pt, ~ 2%) was applied to cover the surface and react with the double bonds for 24 h. The surface with PDMS coating was then soaked in toluene bath for 2 h to remove the unreacted residues.

4.3. Characterization

The surface morphology was characterized by an Auriga (Zeiss) FIB-SEM system. The static, advancing and receding contact angles were

measured using a Drop Shape Analyzer (Krüss, DSA100S). The sliding angles were recorded using the Drop Shape Analyzer (Krüss, DSA100S) with the tilting-plate method based on 20 μL droplets. The chemical compositions of the functionalized surfaces were detected by X-ray photoelectron spectroscopy (XPS, AXIS Supra, Shimadzu). The impact dynamics of droplets were recorded by a high-speed camera (VEO 710L, Phantom) at 10,000 fps. Deionized water drops with various diameters were generated from a micro syringe pump (Longer Precision Pump Co., Ltd, TJ-1A/L0107-1A) equipped with a series of fine needles. Note that except for the experiments in Fig. 2c, all other impacting experiments were based on drops with a uniform diameter of 2.15 mm. The drop impact velocities, contact diameters, dynamic contact angles, contact time, spreading time and retraction time were determined and analyzed from the recorded movies using a custom-programmed MATLAB (Math_Works Inc., USA) algorithm. All the experiments of drop impact were conducted at room temperature with ~ 50% relative humidity.

Declaration of Competing Interest

The authors declare that they have no known competing financial interests or personal relationships that could have appeared to influence the work reported in this paper.

Acknowledgements

This work is supported by National Natural Science Foundation of China (21872176, 22072185, 21805315, 12072381), Pearl River Talents Program (2017GC010671) and Natural Science Foundation of Guangdong Province (2019A1515012030).

Appendix A. Supplementary data

Supplementary data to this article can be found online at https://doi.org/10.1016/j.cej.2022.137638.

References

[1] L. Feng, S. Li, Y. Li, H. Li, L. Zhang, J. Zhai, Y. Song, B. Liu, L. Jiang, D. Zhu, Superhydrophobic surfaces: from natural to artificial, Adv. Mater. 14 (24) (2002) 1857–1860.
[2] R. Blossey, Self-cleaning surfaces-virtual realities, Nat. Mater. 2 (5) (2003) 301–306.
[3] F. Geyer, M. D'Acunzi, A. Sharifi-Aghili, A. Saal, N. Gao, A. Kaltbeitzel, T.-F. Sloot, R. Berger, H.-J. Butt, D. Vollmer, When and how self-cleaning of superhydrophobic surfaces works, Sci. Adv. 6 (3) (2020) eaaw9727.
[4] M. Song, J. Ju, S. Luo, Y. Han, Z. Dong, Y. Wang, Z. Gu, L. Zhang, R. Hao, L. Jiang, Controlling liquid splash on superhydrophobic surfaces by a vesicle surfactant, Sci. Adv. 3 (3) (2017) e1602188.
[5] A.K. Dickerson, P.G. Shankles, N.M. Madhavan, D.L. Hu, Mosquitoes survive raindrop collisions by virtue of their low mass, Proc. Natl. Acad. Sci. U.S.A. 109 (25) (2012) 9822–9827.
[6] L. Wang, R. Wang, J. Wang, T.-S. Wong, Compact nanoscale textures reduce contact time of bouncing droplets, Sci. Adv. 6 (29) (2020) eabb2307.
[7] S. Kim, Z. Wu, E. Esmaili, J.J. Dombroskie, S. Jung, How a raindrop gets shattered on biological surfaces, Proc. Natl. Acad. Sci. U.S.A. 117 (25) (2020) 13901–13907.
[8] L. Mishchenko, B. Hatton, V. Bahadur, J.A. Taylor, T. Krupenkin, J. Aizenberg, Design of ice-free nanostructured surfaces based on repulsion of impacting water droplets, ACS Nano 4 (12) (2010) 7699–7707.
[9] T. Maitra, M.K. Tiwari, C. Antonini, P. Schoch, S. Jung, P. Eberle, D. Poulikakos, On the nanoengineering of superhydrophobic and impalement resistant surface textures below the freezing temperature, Nano Lett. 14 (1) (2014) 172–182.
[10] V. Vercillo, S. Tonnicchia, J.M. Romano, A. García-Girón, A.I. Aguilar-Morales, S. Alamri, S.S. Dimov, T. Kunze, A.F. Lasagni, E. Bonaccurso, Design rules for laser-treated icephobic metallic surfaces for aeronautic applications, Adv. Funct. Mater. 30 (16) (2020) 1910268.
[11] S. Shiri, J.C. Bird, Heat exchange between a bouncing drop and a superhydrophobic substrate, Proc. Natl. Acad. Sci. U.S.A. 114 (27) (2017) 6930–6935.
[12] W. Qi, P.B. Weisensee, Dynamic wetting and heat transfer during droplet impact on bi-phobic wettability-patterned surfaces, Phys. Fluids 32 (6) (2020), 067110.
[13] W. Xu, H. Zheng, Y. Liu, X. Zhou, C. Zhang, Y. Song, X. Deng, M. Leung, Z. Yang, R. X. Xu, A droplet-based electricity generator with high instantaneous power density, Nature 578 (7795) (2020) 392–396.
[14] H. Wu, N. Mendel, D. van den Ende, G. Zhou, F. Mugele, Energy harvesting from drops impacting onto charged surfaces, Phys. Rev. Lett. 125 (7) (2020), 078301.
[15] Z. Ma, J. Ai, Y. Shi, K. Wang, B. Su, A Superhydrophobic Droplet-based magnetoelectric hybrid system to generate electricity and collect water simultaneously, Adv. Mater. 32 (50) (2020) 2006839.
[16] D. Richard, C. Clanet, D. Quéré, Contact time of a bouncing drop, Nature 417 (6891) (2002), 811 811.
[17] J.C. Bird, R. Dhiman, H.-M. Kwon, K.K. Varanasi, Reducing the contact time of a bouncing drop, Nature 503 (7476) (2013) 385–388.
[18] M. Song, Z. Liu, Y. Ma, Z. Dong, Y. Wang, L. Jiang, Reducing the contact time using macro anisotropic superhydrophobic surfaces-Effect of parallel wire spacing on the drop impact, NPG Asia Mater. 9 (8) (2017) e415–e.
[19] Y. Liu, M. Andrew, J. Li, J.M. Yeomans, Z. Wang, Symmetry breaking in drop bouncing on curved surfaces, Nat. Commun. 6 (1) (2015) 1–8.
[20] Y. Liu, L. Moevius, X. Xu, T. Qian, J.M. Yeomans, Z. Wang, Pancake bouncing on superhydrophobic surfaces, Nat. Phys. 10 (7) (2014) 515–519.
[21] D.F. Cheng, C. Urata, M. Yagihashi, A. Hozumi, A statically oleophilic but dynamically oleophobic smooth nonperfluorinated surface, Angew. Chem. 124 (12) (2012) 3010–3013.
[22] D.F. Cheng, B. Masheder, C. Urata, A. Hozumi, Smooth perfluorinated surfaces with different chemical and physical natures: their unusual dynamic dewetting behavior toward polar and nonpolar liquids, Langmuir 29 (36) (2013) 11322–11329.
[23] L. Wang, T.J. McCarthy, Covalently attached liquids: instant omniphobic surfaces with unprecedented repellency, Angew. Chem. Int. Ed. 55 (1) (2016) 244–248.
[24] P. Liu, H. Zhang, W. He, H. Li, J. Jiang, M. Liu, H. Sun, M. He, J. Cui, L. Jiang, Development of "liquid-like" copolymer nanocoatings for reactive oil-repellent surface, ACS Nano 11 (2) (2017) 2248–2256.
[25] A. Hozumi, T.J. McCarthy, Ultralyophobic oxidized aluminum surfaces exhibiting negligible contact angle hysteresis, Langmuir 26 (4) (2010) 2567–2573.
[26] A. Tuteja, W. Choi, M. Ma, J.M. Mabry, S.A. Mazzella, G.C. Rutledge, G. H. McKinley, R.E. Cohen, Designing superoleophobic surfaces, Science 318 (5856) (2007) 1618–1622.
[27] A. Tuteja, W. Choi, J.M. Mabry, G.H. McKinley, R.E. Cohen, Robust omniphobic surfaces, Proc. Natl. Acad. Sci. U.S.A. 105 (47) (2008) 18200–18205.
[28] T.L. Liu, C.-J.-C. Kim, Turning a surface superrepellent even to completely wetting liquids, Science 346 (6213) (2014) 1096–1100.
[29] D.-Y. Kim, J.-G. Lee, B.N. Joshi, S.S. Latthe, S.S. Al-Deyab, S.S. Yoon, Self-cleaning superhydrophobic films by supersonic-spraying polytetrafluoroethylene-titania nanoparticles, J. Mater. Chem. A 3 (7) (2015) 3975–3983.
[30] R.S. Sutar, S.S. Latthe, A. Sargar, C. Patil, V. Jadhav, A. Patil, K. Kokate, A. K. Bhosale, K.K. Sadasivuni, S.V. Mohite, Spray deposition of PDMS/candle soot nps composite for self-cleaning superhydrophobic coating, Macromolecular Symposia, Wiley Online, Library (2020) 2000031.
[31] S.S. Latthe, A.L. Demirel, Polystyrene/octadecyltrichlorosilane superhydrophobic coatings with hierarchical morphology, Polym. Chem. 4 (2) (2013) 246–249.
[32] M.W. Lee, S.S. Latthe, A.L. Yarin, S.S. Yoon, Dynamic electrowetting-on-dielectric (DEWOD) on unstretched and stretched Teflon, Langmuir 29 (25) (2013) 7758–7767.
[33] R.S. Sutar, S.S. Latthe, A. Bhosale, R. Xing, S. Liu, Durable self-cleaning superhydrophobic coating of SiO_2-cyanoacrylate adhesive via facile dip coat technique, Macromolecular Symposia, Wiley Online, Library (2019) 1800218.
[34] M. Rabnawaz, G. Liu, Graft-copolymer-based approach to clear, durable, and anti-smudge polyurethane coatings, Angew. Chem. Int. Ed. 54 (22) (2015) 6516–6520.
[35] W. Chen, A.Y. Fadeev, M.C. Hsieh, D. Öner, J. Youngblood, T.J. McCarthy, Ultrahydrophobic and ultralyophobic surfaces: some comments and examples, Langmuir 15 (10) (1999) 3395–3399.
[36] S. Huang, J. Li, L. Liu, L. Zhou, X. Tian, Lossless fast drop self-transport on anisotropic omniphobic surfaces: origin and elimination of microscopic liquid residue, Adv. Mater. 31 (27) (2019) 1901417.
[37] S. Huang, J. Li, L. Chen, X. Tian, Suppressing the universal occurrence of microscopic liquid residues on super-liquid-repellent surfaces, J. Phys. Chem. Lett. 12 (14) (2021) 3577–3585.
[38] C. Clanet, C. Béguin, D. Richard, D. Quéré, Maximal deformation of an impacting drop, J. Fluid Mech. 517 (2004) 199–208.
[39] J. Eggers, M.A. Fontelos, C. Josserand, S. Zaleski, Drop dynamics after impact on a solid wall: theory and simulations, Phys. Fluids 22 (6) (2010), 062101.
[40] F. Wang, T. Fang, Retraction dynamics of water droplets after impacting upon solid surfaces from hydrophilic to superhydrophobic, Phys. Rev. Fluids 5 (3) (2020), 033604.
[41] X. Li, X. Ma, Z. Lan, Dynamic behavior of the water droplet impact on a textured hydrophobic/superhydrophobic surface: The effect of the remaining liquid film arising on the pillars' tops on the contact time, Langmuir 26 (7) (2010) 4831–4838.
[42] T. Bobinski, G. Sobieraj, M. Psarski, G. Celichowski, J. Rokicki, Droplet bouncing on the surface with micro-structure, Arch. Mech 69 (2017) 177–193.
[43] D. Bartolo, F. Bouamrirene, E. Verneuil, A. Buguin, P. Silberzan, S. Moulinet, Bouncing or sticky droplets: Impalement transitions on superhydrophobic micropatterned surfaces, Europhys. Lett. 74 (2) (2006) 299.
[44] C. Lv, P. Hao, X. Zhang, F. He, Drop impact upon superhydrophobic surfaces with regular and hierarchical roughness, Appl. Phys. Lett. 108 (14) (2016), 141602.
[45] H. Zhan, C. Lu, C. Liu, Z. Wang, C. Lv, Y. Liu, Horizontal motion of a superhydrophobic substrate affects the drop bouncing dynamics, Phys. Rev. Lett. 126 (23) (2021), 234503.
[46] A. Gauthier, S. Symon, C. Clanet, D. Quéré, Water impacting on superhydrophobic macrotextures, Nat. Commun. 6 (1) (2015) 1–6.
[47] R. Zhang, X. Zhang, P. Hao, F. He, Internal rupture and rapid bouncing of impacting drops induced by submillimeter-scale textures, Phys. Rev. E 95 (6) (2017), 063104.

[48] L. Rayleigh, On the capillary phenomena of jets, Proc. R. Soc. London 29 (196–199) (1879) 71–97.
[49] D. Bartolo, C. Josserand, D. Bonn, Retraction dynamics of aqueous drops upon impact on non-wetting surfaces, J. Fluid Mech. 545 (2005) 329–338.
[50] M. Reyssat, D. Richard, C. Clanet, D. Quéré, Dynamical superhydrophobicity, Faraday Discuss. 146 (2010) 19–33.
[51] C. Antonini, F. Villa, I. Bernagozzi, A. Amirfazli, M. Marengo, Drop rebound after impact: The role of the receding contact angle, Langmuir 29 (52) (2013) 16045–16050.
[52] J.W. Krumpfer, T.J. McCarthy, Rediscovering silicones:"unreactive" silicones react with inorganic surfaces, Langmuir 27 (18) (2011) 11514–11519.
[53] D.F. Cheng, C. Urata, B. Masheder, A. Hozumi, A physical approach to specifically improve the mobility of alkane liquid drops, J. Am. Chem. Soc. 134 (24) (2012) 10191–10199.
[54] Y. Chen, X. Yu, L. Chen, S. Liu, X. Xu, S. Zhao, S. Huang, X. Tian, Dynamic poly (dimethylsiloxane) brush coating shows even better antiscaling capability than the low-surface-energy fluorocarbon counterpart, Environ. Sci, Technol, 2021.
[55] J. Sarma, L. Zhang, Z. Guo, X. Dai, Sustainable icephobicity on durable quasi-liquid surface, Chem. Eng. J. 431 (2022), 133475.
[56] L. Zhang, Z. Guo, J. Sarma, W. Zhao, X. Dai, Gradient quasi-liquid surface enabled self-propulsion of highly wetting liquids, Adv. Funct. Mater. 31 (13) (2021) 2008614.